Electrostatics in Biomolecular Structure and Dynamics

MALCOLM E. DAVIS* and J. ANDREW MCCAMMON*

Department of Chemistry, University of Houston, Houston, Texas 77204-5641

Received August 25, 1989 (Revised Manuscript Received February 1, 1990)

Contents

I. Introduction

Electromagnetism is *the* force of chemistry. Combined with the consequences of quantum and statistical mechanics, electromagnetic forces maintain the structure and drive the processes of the chemistry around us and inside us. Because of the long-range nature of Coulombic interactions, electrostatics plays a particularly vital role in intra- and intermolecular interactions of chemistry and biochemistry.

Intramolecular interactions are complicated by quantum mechanical effects. For example, covalent bonds and electron distributions require nonclassical descriptions. Nonetheless, energetics with a strong electrostatic component determine such properties as conformation and dissociation. Polarizability plays an important role in hydrogen bonding. All of this bears on such important considerations as molecular stability and enzymatic activity.

Intermolecular interactions are dominated by electrostatic forces. Understanding of these interactions is importance because encounter is the initial step of biomolecular processes. While some encounters may involve molecules held to a framework that facilitates their approach, more often one, or both, are moving freely in solution. Thus, diffusional encounter of a pair of molecules is the precursor to many biomolecular processes whether the constituents be an enzyme and its substrate, two electron-transfer proteins, DNA and a regulatory protein, or an ion and a channel. Berg and von Hippel[1] review the different forms that the diffusion process can take, while Calef and Deutch[2] review the various theoretical models of diffusion.

An understanding of the initial encounter step is critically important in a number of situations. For example, the diffusion encounter rate sets a limit on the overall reaction rate that further improvements in the chemical efficiency of the participants cannot overcome. For this reason, enzymes whose reactions are diffusion limited have been called "perfected" by evolution.[3] Even in situations where it is not rate limiting, an understanding of the encounter step can be important. For example, it may elucidate orientational behavior important in the chemical reaction. Finally, methods developed to study diffusional encounters can often be used to study equilibrium aspects of pairs of molecules in solution.

Early work was limited to particles moving in potentials with high degrees of symmetry. Computer Brownian dynamics (BD) simulations of diffusional motion have provided the ability to move into a more realistic realm. The basic algorithm of Ermak and McCammon[4] allows the simulation of diffusional motion in much the same way as the molecular dynamics (MD) method allows the simulation of the inertial motion of a set of particles. This algorithm along with further refinements[5-11] has allowed the study of biomolecular systems that often exhibit markedly nonsymmetric geometries and potentials.

The crucial component of these studies is the electrostatic model chosen. In this paper we examine a number of historically successful methods and a number of newer techniques that are coming into their own. Several other reviews provide excellent accounts of various aspects of electrostatics in solution.[12-17] An excellent review on dynamical aspects of reactions involving proteins has been presented very recently by Case.[18]

II. Review of Current Methods

Because of the importance of electrostatic interactions and because of the complications arising from many-body effects, a wide range of techniques have been developed for modeling electrostatic interactions. Their history follows the theoretical and numerical techniques available. From simple pairwise interactions, approaches have been extended to include ion screening and arbitrary geometries. The different methods all have their weaknesses as well as their strengths.

0009-2665/90/0790-0509$09.50/0

Malcolm E. Davis was born in Pittsburgh, PA, in 1960. He obtained a B.S. in physics from Purdue University in 1982. Then, under the guidance of Professor Lonnie L. Van Zandt at Purdue, his thesis research addressed models of DNA–microwave interactions. He was awarded a Ph.D. in 1987 and has since held a postdoctoral position at the University of Houston, working under Professor J. Andrew McCammon, continuing his interest in the physics of biochemical processes.

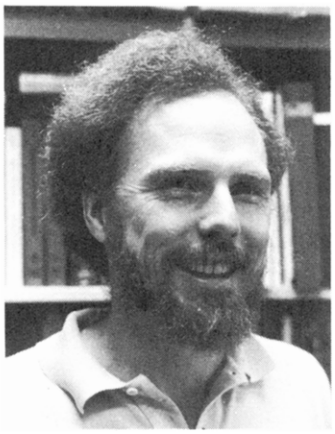

J. Andrew McCammon is the M. D. Anderson Professor of Chemistry at the University of Houston and Adjunct Professor of Physiology and Molecular Biophysics at Baylor College of Medicine. He was born in Lafayette, IN, in 1947. He received his B.A. in chemistry from Pomona College and his M.A. and Ph.D. in physics and chemical physics, respectively, from Harvard University, where he worked with John Deutch on biological applications of statistical mechanics and hydrodynamics. In 1976–1978, he was an NSF and NIH research fellow at Harvard, where he developed the computer simulation approach to protein dynamics in collaboration with Martin Karplus. Since joining the faculty at Houston in 1978, Professor McCammon has developed novel theoretical methods for accurately predicting and interpreting molecular recognition, the rates of diffusion-controlled reactions, and other properties of chemical systems. In addition to their fundamental interest, these methods play a growing role in the design of new drugs, enzymes, receptors, and other materials. Professor McCammon is the author with Stephen Harvey of the book *Dynamics of Proteins and Nucleic Acids*, published in 1987 by Cambridge University Press, and is the author or coauthor of more than 160 papers on a variety of subjects in theoretical chemistry and theoretical biochemistry. He has served on advisory boards for the National Academy of Sciences, the National Science Foundation, the National Institutes of Health, and other agencies. He has also served on the editorial board for several journals. Professor McCammon received the first George Herbert Hitchings Award for Innovative Methods in Drug Design from the Burroughs Wellcome Fund in 1987. He has also been the recipient of an Alfred P. Sloan Fellowship, a Research Career Development Award from the U.S. National Institutes of Health, and a Camille and Henry Dreyfus Teacher–Scholar Award. He is a Fellow of the American Physical Society.

A. Uniform Dielectric Models

That the force between two charges varies inversely with the square of the distance between them was first stated by Joseph Priestly in response to the observation of the absence of charge on the interior surface of a charged, hollow, spherical conductor. Charles Coulomb, whose name has been associated with the law, then verified the behavior through accurate measurements with a torsion balance.[19] It was later discovered that materials, dielectrics, placed between the charges could scale their interaction, reducing the magnitude of the force, but maintaining the relationships to charge and distance. The scaling parameter of the material, the dielectric constant, is a function of the polarizability of the medium, i.e., the ability for dipoles to be induced in the medium. These net dipoles can arise both from the reorientation of permanent molecular dipoles and from intramolecular redistribution of electronic charge. Thus the average behavior of the many-body problem is encapsulated in a single parameter. Application of such a macroscopic quantity in molecular-level calculations is certainly questionable.

The use of a uniform, low dielectric constant is at least a reasonable approximation in MD simulations in which all the solute and solvent atoms are explicitly represented. MD calculations generally ignore intramolecular electronic polarizability and parameterize the permanent dipoles in such a way as to try to compensate for the omission. Some internal polarizability can be incorporated explicitly by using flexible molecular models (i.e., allowing for vibrations).[20,21] Most MD models of liquid water[22] involve rigid molecules, however. The reorientation part of the high polarizability of the solvent is included since the water molecules are treated explicitly, although such models have difficulty producing the correct dielectric constant.[23–28] The use of a uniform, vacuum dielectric constant is, in principle, exact when all contributions to the polarizability are explicitly accounted for. Several groups are currently developing many-body potential functions that treat internal polarizability explicitly.[29–36] The complicated nature of these functions and the need for fitting parameters have limited current usage mostly to small molecular systems. A few applications have been made to proteins, as discussed in section II.C.3.

The use of a single, uniform dielectric constant clearly represents a severe approximation when one considers bulky macromolecules such as globular proteins without an explicit treatment of the solvent. Nonetheless, electrostatics of this form have provided useful insights into the interactions of pairs of molecules too large to be amenable to full-scale MD simulations. Studies of electrostatic complementarity have been quite helpful in examining docked conformations of various proteins.[37,38] Simple charge–charge interaction models have provided insight into the conformations of proteins.[39–45] Qualitative considerations of charge–charge interactions with α-helix dipoles have been used to design protein mutations that enhance stability[46,47] and to explain binding arrangements of proteins and dinucleotides.[48]

Attempts to simulate the solvent by the use of a uniform, large dielectric constant that permeates the solute overestimate the screening of interior charge–charge interactions. The technique, however, has been applied to mapping potential fields around proteins.[49,50]

Calculations by methods that include the lower polarizability of the molecular interior show that the irregular surface of a protein can have a large effect upon the electric potential.[51] Brownian dynamics simulations have shown poor results with uniform dielectric models.[52] They may be of qualitative, but not quantitative utility.

B. Effective Dielectric Constant Models

In attempts to apply Coulomb's law on the molecular level, it is apparent[53] that different pairs of charge sites behave as if they had different effective dielectric constants. Experimentally, effective dielectric constants have been defined[53] on a site–site basis as the expected vacuum electrostatic energy $q_1q_2/4\pi\epsilon_0 r_{12}$ divided by the measured interaction energy, where q_1 and q_2 are the charges at the two sites, ϵ_0 is the vacuum permittivity, and r_{12} is the distance between the sites. The exponential factor of Debye–Hückel theory has also been viewed[54] as an effective dielectric constant. One major difficulty with effective dielectric constants, however, is that their definition is not unambiguous. For example, the exponential Debye–Hückel (DH) factor is differentiated when calculating the electric field, so the effective dielectric constant defined in terms of the force differs from that defined in terms of the energy.

Experimentally, it has been found that the effective dielectric constant in a globular protein generally increases with separation.[53,55] Nearby charges, having little intervening material, can interact almost as in a vacuum if they are not very close to the solvent. More distant charges feel more of the shielding effect due to the solvent surroundings. Attempts have been made to model this behavior[56] with the introduction of a distance-dependent dielectric function that goes from vacuum permittivity at close range to bulk solvent permittivity at large range, with some appropriate switching function in between. The microdielectric method, which will be discussed in section II.D., has been utilized to justify and define such a relation. A simple form, which has been used to advantage in MD simulations, expresses the permittivity as being proportional to separation.[57] Such an expression was advantageous in MD simulations as it turned $1/r$ energy terms into $1/r^2$ terms and $\mathbf{r}/r^3$ force terms into $2\mathbf{r}/r^4$ terms, thus eliminating the need for time-consuming square root calculations in the evaluation of electrostatic forces. While not accurately matching experimental data or more detailed theoretical models,[55,58] the method does permit the inclusion of solvent electrostatic screening, in at least a crude fashion, in cases where the computational load would preclude any more accurate treatment.

An additional method, which can be described as a type of effective dielectric model, scales the charge as a function of distance from the molecular surface.[57,59] Taken to an extreme, some DNA simulations[60] have scaled the phosphate charges to zero. This ad hoc method again crudely includes the solvent screening effects while keeping the calculations to a minimum.

As will be seen in the following sections, the dielectric constant D, or permittivity $\epsilon = D\epsilon_0$, is better associated with regions of space than with sites. Consider the differential form of Gauss's law in an inhomogeneous medium

$$-\nabla\cdot\epsilon(\mathbf{r})\nabla\phi(\mathbf{r}) = \rho(\mathbf{r}) \quad (1)$$

where ϵ is the position-dependent permittivity (which may be a tensor), ϕ is the electrostatic potential, and ρ is the charge density. The permittivity is a measure of the polarizability of regions of space. An additional concern arises from the fact that inhomogeneities in the permittivity lead to stresses on the medium (a matter that will be discussed in more detail below).

C. Heterogeneous Dielectric Models

The first steps in taking continuum models beyond the uniform and effective dielectric descriptions have involved models consisting of a central cavity with associated charges. Original attempts took advantage of as much symmetry and as many limiting approximations as possible to make the problem analytically tractable. Modern computers are pushing back the limitations and allowing more complicated geometries and conditions to be studied.

1. Dielectric Cavity: Born Energy

Perhaps the oldest cavity model is that of Born,[61] which considers the free energy of solvation of a spherical ion immersed in a homogeneous fluid of permittivity ϵ_s. Spherical symmetry reduces the Poisson equation to an ordinary differential equation

$$d^2(r\phi)/dr^2 = r\rho/\epsilon_s \quad (2)$$

In regions where there is no charge the potential then has the form $\phi = C_1/r + C_2$. The constant on the $1/r$ term satisfies Gauss's law, while the constant term provides for continuity of the potential.

The Born model of solvation can be understood either in terms of a uniform dielectric or in terms of a cavity model. In the uniform model the ion of charge q is considered as a sphere of radius a with its charge smeared uniformly over the surface. To satisfy Gauss's law and have the potential vanish as $r \rightarrow \infty$, the potential external to the sphere must be $\phi = q/4\pi\epsilon r$, where ϵ is the permittivity. The total electrostatic energy is $G_B = {}^1/_2\int\rho\phi\, dV$ or $q^2/8\pi\epsilon a$. So the energy change on going from vacuum to solution is

$$\Delta G_B = (q^2/8\pi a)(1/\epsilon_0 - 1/\epsilon_s) \quad (3)$$

where ϵ_0 is the permittivity of free space.

Alternatively, consider the charge q to be a point charge at the center of a solvent exclusion sphere of radius a. The potential external to the sphere is again $\phi = q/4\pi\epsilon r$. Inside the sphere C_1 must be equal to $q/4\pi\epsilon_i$, where ϵ_i is the permittivity of the interior of the ion. To keep the potential continuous, $C_2 = q/4\pi\epsilon a - q/4\pi\epsilon_i a$. The infinite potential at the charge indicates an infinite energy, but this singularity occurs even in a uniform dielectric. The infinity arises because the generation of a mathematical point charge involves bringing finite amounts of charge to zero separation. To avoid the infinite self-energy of creating a mathematical point charge, subtract the uniform dielectric self-potential $q/4\pi\epsilon_i r$ before calculating the energy. The total electrostatic energy is then $G_B = (q^2/8\pi a)(1/\epsilon - 1/\epsilon_i)$. Again, changing the external dielectric surrounding the ion yields the same change in energy as that given in (3). Actually, any spherically symmetric distribution

of charge within the radius a yields the same result.

The Born expression provides a useful measure of the solvation free energy of ions. Obviously the radii can always be chosen ex post facto to match the experimental solvation energy. Latimer et al.[62a] found reasonable fits using crystal radii with corrections for expected solvation structure. Rashin and Honig[62b] have shown that simply choosing the ionic radii for anions and the covalent radii for cations predicts reasonable solvation energies for a wide range of ions. Their choice was based on arguments concerning electron densities in the ions but are similar to Latimer's values. Hirata et al.[62c] have used integral equation techniques, described in section III.B, and found similar cavity radii again grounded in the structure of the solvent.

The Born energy has also been applied[63] to correcting energies in MD calculations which utilize cutoffs in their electrostatic potentials. The cutoff ignores Coulombic interactions beyond a specified radius a. The correction is to assume that the region beyond the cutoff can be treated as bulk solvent. Then, the charge's interaction energy with the solvent beyond a is given by the Born energy ΔG_B. Adding this energy to that calculated explicitly within the cutoff yields the corrected energy. Note, this is a first-order correction ignoring the reaction field from any other charges in the cavity. In addition, the dimensions of large solutes such as proteins approach and exceed the cutoff distance, rendering the assumption of bulk solvent invalid. Therefore, care should be taken in applying this correction.

In the area of intermolecular interactions, the Born model is not an improvement over the uniform dielectric model. The cavities of other molecules cannot be included without destroying the symmetry and thus the simplicity of the solution. The charges of any second molecule can only be treated as test charges in the field of the first molecule. Because of the symmetry, the field outside of the cavity is identical with that for just a point charge in the high dielectric. So the interaction potentials will be identical with those of the uniform dielectric model.

2. Debye–Hückel Model

In 1923, Debye and Hückel published their work[64] on a theory to include the effects of electrolyte ions in the description of electrostatic phenomena in liquids. In polar solvents, an applied field will cause the dipoles to align, which will on average lead to no net charge density in the uniform bulk, but only at boundaries or inhomogeneities in the permittivity. For ionic solutions, however, the charges are not bound as dipoles but have the ability to move freely under the influence of electric fields. Their own interaction and thermal agitation keep them from collapsing onto the boundaries, which leads to net charge densities throughout the bulk solvent.

From statistical mechanics, the ions should be distributed in the solution according to a Boltzmann distribution. The number density of positive and negative ions $n_\pm$ is given by

$$n_\pm = n_\infty \exp(-U_\pm/k_BT) \tag{4}$$

where n_∞ is the bulk number density, $U_\pm$ is the free energy of potential of mean force for a positive or negative electrolyte ion to be at the location of interest, k_B is Boltzmann's constant, and T is the absolute temperature. For a 1:1 electrolyte, adding the local electrolyte charge to the explicit charge ρ makes the differential form of Gauss's law

$$-\nabla\cdot\epsilon\nabla\phi = \rho + en_+ - en_- \tag{5}$$

with e being the unit electrical charge. If one assumes that the energy of the ion is just its charge times the potential, then this becomes a nonlinear differential equation in ϕ, the Poisson–Boltzmann (PB) equation for a 1:1 electrolyte

$$-\nabla\cdot\epsilon\nabla\phi = \rho - 2en_\infty \sinh(e\phi/k_BT) \tag{6}$$

Without the modern advantages of computers, solutions to the nonlinear equation were too hard to obtain. The next approximation, then, was to assume that $e\phi$ was small with respect to k_BT and then take only the linear term in the Taylor series expansion of the hyperbolic sine function. This yields the linearized Poisson–Boltzmann (LPB) equation

$$-\nabla\cdot\epsilon\nabla\phi = \rho - e\kappa^2\phi \tag{7}$$

where, in this case, $\kappa^2 = 2e^2n_\infty/k_BT\epsilon$. More generally in SI units, the Debye–Hückel screening parameter κ is given by $\kappa^2 = Ie^2/k_BT\epsilon$, where I is the ionic strength.

As in the derivation of the Born energy, assume that the "central ion" is a sphere with a charge q at its center. Then if the radius of this sphere is a

$$\phi = \frac{q}{4\pi}\left[\frac{1}{\epsilon_i r} - \frac{1}{\epsilon_i a} + \frac{1}{\epsilon_s a(1+\kappa a)}\right] \qquad r \le a \tag{8a}$$

$$\phi = \frac{q\exp(-\kappa(r-a))}{4\pi\epsilon_s r(1+\kappa a)} \qquad r \ge a \tag{8b}$$

As in the cavity derivation of the Born energy, subtracting out the constant infinite self-energy of the point charge leaves the total free energy of the ion

$$G_{DH} = \frac{q}{4\pi}\left[\frac{1}{\epsilon_s a(1+\kappa a)} - \frac{1}{\epsilon_i a}\right] \tag{9}$$

Differences can then be taken between a given solvation state and the vacuum state ($\epsilon_s = \epsilon_0$ and $\kappa = 0$) to obtain the ionic-strength-dependent solvation energy.

$$\Delta G_{DH} = \frac{q}{4\pi}\left[\frac{1}{\epsilon_s a(1+\kappa a)} - \frac{1}{\epsilon_0 a}\right] \tag{10}$$

Note that again the internal permittivity cancels out in the differences.

For use as an intermolecular potential, it must be noted that, as with the Born model, the potential is not the sum of the individual particle potentials when the cavity radii are nonzero. Mathematically, this results from the fact that the differential equation is not linear in such a combination of particles, because the position-dependent permittivity function also changes. Physically, summing the potentials ignores the interaction of each atom with the polarization charge it induces at the surface of the other cavities. If the radii are zero, then there are no dielectric boundaries. Although this leads to infinite total energies because the self-induced polarization charges collapse to mathematical singularities, this yields a form of the potential for point charges in an ionic solution that is strictly

additive in the manner of the Coulombic interaction.

In BD studies done on the enzyme superoxide dismutase (SOD),[52,65] it was discovered that the neglect of the irregular shape of the exclusion volume led to predicted reaction rates that are significantly different from those observed. The convolutions of the dielectric and ion exclusion boundaries lead to focusing of the electrostatic potential in the solvent that affects the steering of the substrate to the active site of the enzyme. In situations where such focusing effects are not important, or where computational efficiency demands, the Debye–Hückel potential for a spherical central ion still serves as an important first approximation. But with the simplified geometry there is a certain arbitrariness about the definition of reactive patches on the spheres, which permits a large range of reaction rates to be predicted with reasonable parameters.

3. Kirkwood–Westheimer–Tanford Model

Kirkwood[66] generalized the Debye–Hückel model by considering charge distributions in the cavity that were not spherically symmetric. Kirkwood and Westheimer then applied this method to calculate dissolution constants of organic acids, with models for both spherical and ellipsoidal cavities.[67,68] The later extensions have been primarily applied to the simpler spherical model, so we will restrict our considerations to that model here.

In regions with no explicit charge, the LPB equation becomes Laplace's equation inside the ion spherical exclusion cavity (radius a) and Helmholtz's equation in the solvent.

Therefore, for a point charge q at $\mathbf{r}_0$, the potential must have the form

$$\phi = q/(4\pi\epsilon_i|\mathbf{r} - \mathbf{r}_0|) + \sum_{l=0}^{\infty}\sum_{m=-l}^{l} A_{lm} r^l Y_l^m(\theta,\phi) \quad r < b \tag{11a}$$

$$\phi = \sum_{l=0}^{\infty}\sum_{m=-l}^{l} (B_{lm} r^l + C_{lm} r^{-l-1}) Y_l^m(\theta,\phi) \quad b < r < a \tag{11b}$$

$$\phi = \sum_{l=0}^{\infty}\sum_{m=-l}^{l} D_{lm} \frac{K_l(\kappa r)\exp(-\kappa r)}{r^{m+1}} Y_l^m(\theta,\phi) \quad r \geq a \tag{11c}$$

where K_l are the modified spherical Bessel functions and Y_l^m are spherical harmonics. Expanding $1/|\mathbf{r} - \mathbf{r}_0|$ in terms of spherical harmonics allows the boundary conditions at the dielectric discontinuity b and the ion exclusion radius a to be applied term by term to determine the coefficients.

For a collection of N charges the potential is the sum of the individual potentials since the equation is linear. The energy is therefore

$$W = W_{cc} + W_{cs} + W_{ci} \tag{12}$$

where (in SI units)

$$W_{cc} = \frac{1}{2}\sum_{j=1}^{N}\sum_{k\neq j}\frac{q_j q_k}{4\pi\epsilon_i r_{jk}} \tag{13}$$

is the charge–charge interaction energy (r_{jk} is the distance separating charge j and charge k),

$$W_{cs} = \frac{1}{2}\sum_{j=1}^{N}\sum_{k=1}^{N}\frac{q_j q_k}{4\pi\epsilon_i b}\sum_{n=0}^{\infty}\frac{(n+1)(\epsilon_s - \epsilon_i)}{(n+1)\epsilon_s + n\epsilon_i}\left(\frac{r_j r_k}{b^2}\right)^n P_n(\cos\theta_{jk}) \tag{14}$$

is the energy from the interaction of the charges j with induced polarization charge at the solvent interface from charges k (θ_{jk} is the angle between $\mathbf{r}_j$ and $\mathbf{r}_k$, and P_n are the Legendre polynomials), and

$$W_{ci} = \frac{1}{2}\sum_{j=1}^{N}\sum_{k=1}^{N}\frac{q_j q_k}{4\pi\epsilon_i a}\left[\frac{\kappa a}{1+\kappa a} + \sum_{n=1}^{\infty}\frac{2n+1}{2n-1}\left(\frac{\epsilon_s}{(n+1)\epsilon_s + n\epsilon_i}\right)^2 \times \left(\frac{(\kappa a)^2 (r_j r_k/a)^n P_n(\cos\theta_{jk})}{\frac{K_{n+1}(\kappa a)}{K_{n-1}(\kappa a)} + \frac{n(\epsilon_s - \epsilon_i)}{(n+1)\epsilon_s + n\epsilon_i}\left(\frac{b}{a}\right)^{2n+1}\frac{(\kappa a)^2}{4n^2-1}}\right)\right] \tag{15}$$

is the energy from the interaction of the charges with the net charge density induced in the ion distributions.

Tanford and Kirkwood[69–71] applied this method to proteins in 1957 to determine protein titration curves. To arrive at a calculable form for these systems with multiple titratable groups, they assumed that $\epsilon_s \gg \epsilon_i$, that all of the charges were at the same depth, and that identical residues had identical pK_a values. The average contribution to the free energy from all configurations was then approximated as a series in the statistical moments of the distribution of the energies of the different configurations. Tanford and Roxby[72] noted difficulties in the method for accurate calculation of pK_a values of individual groups when applied to proteins.

An ad hoc method for accounting the irregular shape of the protein was introduced by Shire et al.,[73,74] who used a scaling factor that depends on the solvent accessibility of each charged residue. The new interaction energy W'_{ij} between charges i and j is given by

$$W'_{ij} = (1 - \overline{SA_{ij}})W_{ij} \tag{16}$$

where W_{ij} is the standard Tanford–Kirkwood (TK) interaction energy and $\overline{SA_{ij}}$ is the average of the fractional solvent accessibilities of the sites i and j. This form has been used successfully to calculate titration curves for globular proteins.[13,58]

While it does provide a scheme for including the extra shielding that a surface charge will have, the solvent accessibility factor seems questionable for intermolecular potentials. Such a scaling seems to imply that a charged residue that extends out into the solvent could have a smaller effect on the field in the solvent surrounding it than would a more distant buried charge. Nonetheless, electrostatic complementarity, the matching of positive to negative regions during binding of enzyme and substrate, has been found in several systems utilizing this method.[13,75]

An alternative inclusion of solvent accessibility developed by States and Karplus appeared in an application to hydrogen exchange behavior by Delepierre et al.[76] By using actual charge positions obtained from X-ray crystallography and defining the radius of the cavity as the radius at which the protein density drops

to half of its central value, they position some charges in the solvent, where they are more strongly shielded from the interior. This will also provide an approximate model for intermolecular interactions. However, it will still not include the focusing effects found so important in the studies of SOD.

Other modifications include the Head-Gordon and Brooks[77] rederivation which provides a form for simpler calculation and extensions by van Faassen et al.[78] which smooth the dielectric discontinuity.

In addition to the applications to titration curves and complementarity mentioned above, the Kirkwood–Westheimer (KW) cavity model has been used widely because of its analytic form. It has been utilized for calculations of properties ranging from electron-transfer rates,[79] to electrostatic free energies of proteins,[80] to potential functions for BD simulations.[81,82]

4. Finite Element Methods

Orttung[83] moved beyond the simple geometry cavity by exploiting the finite element method for solving differential equations. The finite element method was developed by engineers studying mechanical stress problems but has become a method widely used in many disciplines.[84,85] In this method, space is divided into a collection of small domains, the finite elements, on which the solution is assumed to have a very simple form of only a very limited number of terms in a power series. For example, on a triangular element the solution could be expanded in terms of three functions, each of which has value one at one corner (node) and zero at the other two. To improve the accuracy, rather than include more terms in the expansion, the space is merely divided into smaller elements.

The solution of Poisson's equations in terms of these functions, coupled with the boundary conditions with adjacent elements, leads to a large system of linear equations in the coefficients of these functions. For the functions cited above, the coefficients are just the potentials at the nodes. Many tricks have been implemented in finite element packages to optimize solving these systems. For example, the numbering of the elements can be reordered to move all of the nonzero coefficients close to the diagonal, producing a banded matrix with the narrowest possible width. This optimizes the system for both storage and solution.

Dividing the space into elements is a major task. Much work has been done in developing algorithms for tiling two dimensions with triangles and rectangles. The problem is even harder in three dimensions, but algorithms are available; see, for example, refs 86 and 87. Research continues on a posteriori error analysis,[88,89] which can be used in mesh refinement.

The finite element method permits the description of arbitrary geometry, with high accuracy. Much of the work with this technique in engineering has utilized systems that were reducible to two dimensions, but three-dimensional calculations are increasing. Probably the largest deterrent to the use of finite element methods is the difficulty of implementation. The algorithms are more complicated than the finite different methods described in the next section. The complexity in the grid generation is coupled with the complexity of the bookkeeping. Finding the potential at an arbitrary point after the solution has been determined is not as trivial as it is in the finite different approximation to be discussed next.

In the area of molecular electric fields, this methodology has been principally applied to small atomic and molecular systems.[17] The prime concern has been determining realistic local values for ϵ as a function of position in molecules. Orttung and co-workers have written several papers[90–93] that examine the local dielectric constant. They determine the local value of ϵ from quantum mechanical considerations, since ϵ is just a measure of the polarizability of the medium, i.e., the electronic distribution in this case.

Although most of the work with this method has not incorporated counterions, there is no inherent restriction in the method. Code for solving the Poisson equation is probably more readily available, however, as it figures prominently in solid mechanics calculations and electrical engineering studies of antennas and resonant cavities.

5. Finite Difference Methods

Warwicker and Watson[94] applied the method of finite differences to the problem of electrostatics around an irregular cavity. In this method, space is divided into a regular (usually rectangular) grid of points, and derivatives are approximated as differences between the values of the function at these points. The most physically illuminating method for deriving the finite difference form for the LPB equation is to integrate the equation over the small box around each grid point and utilize the divergence theorem

$$-\oint_S \epsilon \nabla\phi \cdot d\hat{S} + \int_V \epsilon\kappa^2\phi \, dV = \int_V \rho \, dV \qquad (17)$$

The normal of $\epsilon\nabla\phi$ is assumed to be constant over each face and to be approximated by the value of ϵ assigned to the face times the difference in the potential at the grid points on each side of the face, divided by the grid spacing. The value of $\epsilon\kappa^2$ is considered to be constant over the volume and the potential is taken as that of the grid point at the center of the box. This reduces the integrodifferential equation to a set of difference equations

$$h^2 \sum_{j=1}^{6} \epsilon_{ij}(\phi_i - \phi_j)/h + c_i h^3 \epsilon\kappa^2 \phi_i = q_i \qquad (18)$$

where j runs over the six grid points adjacent to grid point i, ϵ_{ij} is the permittivity of the face connecting i and j, c_i is the fraction of the volume accessible to counterions, and q_i is the charge enclosed.

The values of ϵ for the grid faces are generally assumed to be either that of the solvent or of the interior, based on some criteria for defining the surface. For example, ϵ may be set to the internal permittivity if the midpoint of the line connecting the faces is within the van der Waals radius of the particular atom, and to the solvent permittivity otherwise. Similarly, various methods are available for assigning charges to the grid. The earliest attempts put the entire charge of an atom on the nearest grid point. With the grid spacing typically on the order of 1 Å, this leads to rather large shifts in the relative positions of charges. Edmonds et al.[95] developed a scheme by which the charge is spread over the eight nearest grid points by a trilinear weighting function, which minimizes the errors in the lowest

moments of the charge distribution. Gilson et al.[96] have developed a different scheme that minimizes the error in the center of charge.

Advantages of the finite difference methods include the straightforward and physically transparent nature of the calculation and the ease of obtaining values for the field at arbitrary points. Its primary disadvantage has been its computational intensity. In addition, placing the molecule on the grid can produce a rather crude representation of the surface and charge locations. We will discuss some improvements to this assignment in section III.

Finite difference methods have now been used extensively in BD simulations of SOD,[52,65,97] heme proteins,[6,98] and triose phosphate isomerase.[99] They have been used to calculate pK_a shifts,[100,101] conformational[94,102,103] and binding energies,[103] redox potentials,[104] recognition potentials and interaction energies,[105-108] and the role of electrostatics in enzymatic mechanisms.[109]

6. Boundary Element Methods

Any system with multiple dielectrics can be replaced by an equivalent uniform dielectric problem with appropriate surface charges σ at the dielectric boundaries. Levitt[110] applied such a technique to systems with cylindrical symmetry, which reduces the determination of σ to a one-dimensional problem. Zauhar and Morgan[111,112] have extended the method to arbitrary geometries. This method is similar to a finite element method, but only elements in the two-dimensional region of the interface need to be considered. Conceptually, the problem of determining the electric potential function for charges in an irregular low-dielectric cavity in a high-dielectric solvent is replaced by the problem of determining the charges that would produce the same potential function in a vacuum. To get the $q/4\pi\epsilon_i r$ singularities at the actual charges, the charges q are replaced by q/ϵ_i. The discontinuity in the normal component of the field at the dielectric boundary is replaced by a surface charge density

$$\sigma = \frac{\epsilon_i - \epsilon_s}{\epsilon_i}\mathbf{E}\cdot\hat{n} \tag{19}$$

where $\mathbf{E}$ is the field on the solvent side of the boundary and $\hat{n}$ is the outward unit normal. (Again note the use of SI units rather than the Gaussian units of the original papers.)

The finite element method is employed to determine the surface charge density. The surface is divided into triangular elements, so that the charge on each element becomes an unknown in a system of linear equations. With the solution of the system of equations, the potential at any arbitrary point is just the sum of the Coulomb potentials for the *all* of the charges, explicit and polarization.

In a region of high dielectric constant, such as the solvent surrounding a target protein, the explicit and polarization charges generate large canceling contributions. To avoid the numerical inaccuracies inherent in such a calculation, Zauhar and Morgan developed a variation in which the solution for a perfectly conducting solvent, $\epsilon = \infty$, is subtracted out of the system and then the difference in the polarization charge for the real solvent is calculated. The external field is produced just by this differential polarization charge.

Rashin and Namboodiri[113] utilize a similar technique but take a more simplified view of the method. Drummond[114,115] uses a supertensor formalism to achieve a related approach.

Since only a two-dimensional mesh is required, this method can describe the molecular surface much more accurately for a given number of equations than can finite element or finite difference methods. In addition, charges are placed exactly as point charges and not spread over grid points as in the finite difference method.

The inclusion of ionic strength effects is difficult, however, because spectator ions produce a volume distribution of charge. Inclusion of the volume charge effects when only the dielectric interface is explicitly considered requires the knowledge of a type of Green function for the irregular cavity. Methods for boundaries with simple geometries exist, but solving for such a Green function in the general case is essentially what the finite element and finite difference methods do.

The cylindrically symmetric formulation has been applied by Levitt[110] and Jordan.[116-120] The method has been applied to the fields around some small molecules[111] and lysozyme[112] as well as to hydration enthalpies.[113,121] It has not, to our knowledge, yet been applied to BD simulations.

7. Image Methods

Another method for handling discontinuities is the method of images.[122] Consider a charge q near a grounded plane conductor. It can easily be seen that the potential on the front side of the conductor (the side toward the charge) is equivalent to the potential that would exist if the conductor were replaced by a charge of $-q$ the same distance behind the conductor as the actual charge is in front, analogous to a mirror image.

This ability to replace boundaries with "image" charges is not limited to this simple geometry or to conductors. If the conductor ($\epsilon = \infty$) is replaced by a semiinfinite dielectric (finite ϵ), the potential on the front side of the boundary is equivalent to that of the actual charge q plus a charge of $-q(\epsilon - \epsilon_0)/(\epsilon + \epsilon_0)$ at the same distance behind the boundary. Behind the boundary, the potential is equivalent to that of a single charge q/ϵ at the position of the original charge.

For spherical conductors a simple image can also be obtained. It has charge $-qa/r_0$ at radius a^2/r_0, where a is the cavity radius and r_0 is the radial position of the actual charge. For spherical dielectrics, however, an infinite progression of images is necessary to match the boundary condition at the surface, for, in a sense, the image that is created by one surface of the sphere creates an image in the far surface, much as facing mirrors produce an infinite sequence of images. However, as an approximation, the same charge scaling as occurred in going from the conductor to dielectric in the plane case can be applied, yielding an approximate image charge of

$$q' = -\left(\frac{\epsilon_i - \epsilon_s}{\epsilon_i + \epsilon_s}\right)\frac{a}{r_0}q \tag{20}$$

The approximate solution for a collection of charges is

just the collection of charges plus their individual images.

This approximation moves cavity electrostatics into the realm of pairwise interactions, with the computational advantages that entail. Such advantages are primarily of value in Monte Carlo (MC) and MD simulations. For other applications, the accuracy of the full series solution may be more important than the computational efficiency of the image approximation. The main application for spherical cavities in MC and MD simulations is as a boundary condition. Allen and Tildesley[22] describe the implementation of the image charge method as a boundary condition for such simulations.

Shaw[123,124] has developed an analytic approximation for the surface charge theory that underlies the boundary element method. The latest work improves upon the accuracy by including approximate image charges, or quasi-images, along with a surface charge contribution. The quasi-image is the image charge that the original charge would generate in a sphere that would match the curvature of the nearest surface.

As with the boundary element method, including ionic strength effects presents a problem except when the boundary geometry is simple. It is interesting to note, however, that the ions will only serve to make the solvent more like a perfect conductor and so improve the validity of the basic image approximation, but it is not clear how such a scheme might be implemented for arbitrary boundaries. In special cases, Green functions can be determined analytically that will allow the potential everywhere to be determined from the equivalent of a surface charge at the boundary, but for such geometries direct analytic methods (e.g., series expansion) exist for calculating the potential as well.

D. Inducible Dipole Models

An alternate representation of the polarizability involves modeling inducible point dipoles. In such methods the field due to the explicit charges is calculated with no induced dipoles. The induced dipoles are then calculated as the field times the local polarizability, and then new total fields are calculated. Iteration can be performed to convergence.

This representation is roughly equivalent to a spatially dependent dielectric constant. A sphere of radius a and permittivity

$$\epsilon = \epsilon_0\left(1 + \frac{3\alpha}{4\pi\epsilon_0 a^3 - \alpha}\right) \tag{21}$$

will produce a field outside the sphere equivalent to an inducible point dipole of permittivity α (SI units) when subjected to a uniform applied field. Integration of the polarization $\mathbf{P}$ over the volume shows that the dipole moment is equivalent.

Warshel has modeled protein–solvent systems as a set of inducible point dipoles. In this microdielectric model, the solvent is treated as an explicit set of dipoles located at fixed positions, whose polarization is determined through energy minimization. Distant waters are placed on a cubic grid and are also inducible. The method includes electronic polarization of the protein by a similar induced-dipole treatment and orientational polarization of the protein by nuclear displacement. The static nature of the solvent structure, attributing all of the polarizability of the solvent to inducible dipoles, has attracted criticism, as has the arbitrary location of the distant waters.[125] It may be possible, however, that proper parameterization of the polarizability permits a mimicking of the solvent behavior. Warshel has used the model to develop a distance-dependent dielectric constant formalism that, as discussed before, leads to greater computational simplicity than the iterative scheme entails. The methodology has been applied primarily to intramolecular studies, for example, structural stabilization[126] and pK_a calculations.[127]

Pollock and Alder[24] used inducible dipole models in MD studies of polarizable liquids. A similar representation of inducible dipoles has been applied to MD simulations of proteins by Van Belle et al.[128] In these, all solvent molecules are mobile, avoiding some of the problems of the microdielectric method. Their calculations on three proteins showed that the polarizability contributes to stabilization in ways that are not accounted for in terms of a uniform low dielectric protein interior or by distance-dependent dielectric models. The added degrees of freedom lead to longer computational times in order to reach convergence. Typically about eight iterations are required for the fields to converge.

It is important to note that potential energy functions will need to be reparameterized when polarization is included explicitly (as they must for any change in electrostatic model), since typical parameterizations have been skewed to artificially match experimental quantities without the inclusion of polarizability.[35,36,129]

E. Hybrid Methods

The particle–particle/particle–mesh (PPPM) method[22] calculates short-range forces with pairwise additive Coulombic interactions, while the long-range interactions of the charges with all of their periodic images are calculated by a mesh technique. The mesh technique positions all of the charge on a grid as in the Warwicker and Watson algorithm.[94] In this system a uniform dielectric is assumed and so the potential on the periodic grid can be determined by using fast Fourier transforms. It is a numerical alternative to performing an Ewald sum.[22,130]

Nakamura[131] has developed a variation that involves a hybridization of the mesh techniques of Warwicker and Watson for a spherical cavity and explicit charge–charge interactions. This is similar to reaction field corrections for simulations in a finite spherical box.[63] The reaction field is calculated numerically, rather than with an analytic approximation.

Nakamura divides space into two regions. In the first, solute and solvent are treated explicitly. This region occupies a spherical cavity in the second region, which is treated as continuum solvent. The reaction field is calculated as the difference between the potential with the continuum as solvent and the continuum as vacuum. The charge–charge interactions are then included with Coulomb's law. As with the energy methods utilized by Gilson and Honig,[103] this two-step process eliminates the self-energy of creating each of the charges individually in an infinite medium of permittivity ϵ_i.

III. Perspective

We have presented some of the more standard methodologies. In this section, we discuss some of the areas for improvement in these techniques. In addition, we examine some additional techniques that, while not necessarily new, are new to the realm of biomolecules. The outlook for overcoming many of the difficulties discussed previously is encouraging.

A. Improvements to Finite Difference Methods

The finite difference method for solving the LPB equation has become widely utilized. One of the impediments to its more widespread application has been the heavy computational demands of these calculations. Recent work by the authors[132] has shown that application of different numerical techniques developed for sparse matrix inversion[133] can provide a significant improvement over the usual relaxation techniques for solving the LPB on a nonvector machine, although storage requirements are increased by a third. For a fixed amount of computer memory this reduces each grid dimension by 9%, or typically three grid points off each side. The application of these numerical techniques is made possible because of the very regular structure of the coefficient matrix for the system of equations being solved. The coefficient matrix is sparse and the nonzero elements occur in specific sub and super diagonals. (In the finite element and boundary element methods, the matrix is sparse and elements can be reordered to move the nonzero elements near to the diagonal, but they do not form the orderly structure obtained in the finite difference methods.) Vector and parallel optimization hold promise for even greater speed.[134-136]

Another shortcoming of current cavity methods has been that for intermolecular (and for some intramolecular) interactions, the test charge approximation is utilized. The electric potential ϕ is first calculated from a given charge distribution and dielectric boundary. The charges that interact with this potential are then treated as test charges; i.e., their energy is $q\phi$ and their force is $-q\nabla\phi$. The test charge approximation assumes that the charges are small enough not to disturb the charge distributions generating the field. With inhomogeneous dielectrics this is not necessarily the case. The reaction field generated by these charges is not always negligible.[137]

A finite rectangular grid is not always the most natural geometry. Extensions from simple rectangular grids are also being made. In their calculations of fields around DNA, Jayaram et al. implemented periodic boundary conditions along the helix axis to get the fields for an infinite molecule.[138] Jordan et al.[139] have exploited cylindrical grids for the study of ion channels. Currently, the authors are working on the implementation of a spherical grid.

The linearization of the PB equation is another area of concern. The approximation that $e\phi$ be small with respect to k_BT is not always valid, especially when considering such highly charged species as nucleic acids. Jayaram et al.[138] in their finite difference calculation of the fields around DNA have included terms beyond the linear in the expansion of the sinh $(e\phi/k_BT)$ factor in eq 6. Allison et al.[140] and Bacquet et al.[141] have seen significant differences between linearized and nonlinearized PB potentials in protein systems as well. Inclusion of the nonlinear terms in the finite difference calculations is not, however, a trivial matter. In addition to the cost of calculating the additional terms, the nonlinearity introduces instability into the relaxation techniques. To get convergence it sometimes is even necessary to use underrelaxation rather than overrelaxation to achieve convergence. Finally, there are some difficulties with the energy no longer being uniquely defined in the nonlinear form of the equation.[142]

One concern in all of the cavity methods is the value of the dielectric constant to be used for the protein interior. Gilson et al.[143] provide an insightful discussion concerning the nature of this problem. The redistribution of charge in a molecule as the result of an applied field can arise from electronic polarizability as well as the reorientation of charge-bearing groups. Similations of flexible molecules need only account for the electronic polarizability. In rigid systems, the local dielectric constant must account also for the reorientation effects. Note that utilization of such a dielectric constant assumes that the response to the field is linear. In situations where large conformational changes can take place, it may not be possible to model the response in this fashion and flexibility will have to be included explicitly.

In principle, it should be possible to refine the uniform cavity model to include the variation of polarizability throughout a molecule. The application of a uniform field $\mathbf{E}$ to a sphere of radius a and permittivity ϵ induces a polarization charge on the sphere equivalent to a point dipole of $\alpha\mathbf{E}$, where

$$\alpha = 4\pi a^3\epsilon_0(\epsilon - \epsilon_0)/(\epsilon + \epsilon_0) \qquad (22)$$

with the polarizability α in SI units (α(SI) = $4\pi\epsilon_0\alpha$-(Gaussian)). For nonuniform fields, the results would be different since the sphere would feel a range of fields, while the point dipole only feels the field at the center. This is not necessarily a problem, since the ability to model variations in the field is often modeled with induced multipoles; see, for example, Oxtoby.[144] In addition, techniques such as including inducible dipoles at bond midpoints reflect the spatial dependence of the polarizability of the intramolecular medium.

The assignment of the permittivity to local regions within a cavity is not unambiguous. The permittivity within the volume of each atom could be set to the value appropriate for a sphere, with the overlap regions divided between the atoms. Or in the manner of the bond dipoles, the overlapping regions could be empirically parameterized to some combination. Nakamura et al.[145] examined a method using spherical averaging, including electronic and orientational polarization through atomic polarizabilities and the fluctuation–dissipation theorem. Adoption of radial polarizability functions (see, for example, Ehrenson[146]) provides an alternative approach. Of course, the most rigorous modeling would follow the work of Orttung and co-workers[90-93] and approach the problem from a quantum mechanical standpoint. As pointed out by Harvey,[17] the errors inherent in other parts of the treatment may obviate the need for extreme accuracy in the polarizability at the present time.

B. Beyond the Poisson–Boltzmann Equation

Methods such as the reference interaction site model (RISM) integral equations offer means to move beyond the approximations of the PB equation.[147] Specifically, the energy that should appear in the Boltzmann distribution should be the potential of mean force rather than just the electrostatic energy $q\phi$. Short-range interactions and ion–ion correlations are neglected in the PB approach.

The RISM approach derives from pair correlation theory. The total pair correlation $h(\mathbf{r}_1,\mathbf{r}_2)$ is the direct correlation $c(\mathbf{r}_1,\mathbf{r}_2)$ of finding an atom at $\mathbf{r}_1$ given one at $\mathbf{r}_2$; plus the probability of finding an atom at $\mathbf{r}_1$ correlated with an atom at $\mathbf{r}_3$ while that particle is correlated with an atom at $\mathbf{r}_2$ integrated over all possible $\mathbf{r}_3$; plus triple pairs; and so on. That is

$$h(\mathbf{r}_1,\mathbf{r}_2) = c(\mathbf{r}_1,\mathbf{r}_2) + \int \rho c(\mathbf{r}_1,\mathbf{r}_3)c(\mathbf{r}_3,\mathbf{r}_2)\, d\mathbf{r}_3 + \int \rho^2 c(\mathbf{r}_1,\mathbf{r}_4)c(\mathbf{r}_4,\mathbf{r}_3)c(\mathbf{r}_3,\mathbf{r}_2)\, d\mathbf{r}_4\, d\mathbf{r}_3 + \ldots \quad (23)$$

where ρ is the particle density. Combining the integrals and factoring out the integral over $\mathbf{r}_3$ leaves an integral factor equivalent to the original expression and therefore equal to $h(\mathbf{r}_3,\mathbf{r}_2)$, yielding the Ornstein–Zernicke (OZ) equation

$$h(\mathbf{r}_1,\mathbf{r}_2) = c(\mathbf{r}_1,\mathbf{r}_2) + \int \rho c(\mathbf{r}_1,\mathbf{r}_3)h(\mathbf{r}_3,\mathbf{r}_2)\, d\mathbf{r}_3 \quad (24)$$

This coupled set of integral equations relates the total pair correlation function h and the direct pair correlation function c. To solve this system of integral equations a closure relation is required.

The hypernetted chain (HNC) technique applies the approximate closure relation

$$h = \exp[-(u/k_BT) + h - c] - 1 \quad (25)$$

where u is the effective pair potential and the $h - c$ terms in the exponential add correlation effects to the standard Boltzmann factor. With these more accurate descriptions of the distribution of spectator ions (and solvent molecules, if these are included explicitly), more accurate potentials of mean force can be calculated in principle for the solute displacements of interest (intra- or intermolecular).

Such methods have been useful in the study of polar liquids,[147] ionic solutions,[148] dipeptides,[149] ionic colloidal solutions,[150] and simple models of biopolymers at infinite dilution.[151,152] Hirata and Levy have applied this technique to a string-of-pearls model for DNA and found reasonable results for the B–Z transition dependence on ionic strength.[153] Murthy et al.[154] have compared PB, HNC, and MC approaches to ion distributions around an infinite circular cylinder model of DNA. Bacquet et al.[141] have done the same for a protein model. Their results indicated that the HNC distributions matched those from the MC calculations better than the PB distributions. This approach has been limited, however, to infinite dilution because inaccuracies arise in interactions between polyelectrolytes.[155] As with the MD simulations, HNC calculations fail to accurately calculate the dielectric constant of water.

Alternatively, the PB equation can be modified to include ion–ion correlations.[156–159] This approach has been primarily directed at electric double-layer problems and applications to micellar solutions.[160,161]

C. Quantum Mechanics

An entirely different frontier lies in the realm of quantum mechanical calculations. Even if methods for modeling the spatial dependence of the permittivity are developed, they are just that, models of the underlying quantum mechanical behavior of the molecules. The distributions of electrons in molecules are determined by the time-independent Schroedinger equation for the electrons and nuclei, which interact with a Coulombic potential

$$\left[-\sum_i \frac{h^2}{8\pi^2 m_i}\nabla_i^2 + \sum_i \sum_{j<i} \frac{q_i q_j}{4\pi\epsilon_0 r_{ij}}\right]\Psi = E\Psi \quad (26)$$

where h is Planck's constant, m_i is the particle mass, and Ψ is the molecular wave function. The summations run over all of the nuclei and electrons in the molecule. Ab initio techniques[162,163] are used to solve this eigenvalue equation in various levels of approximation. Then

$$\phi(\mathbf{r}) = \sum_{i=\text{nuclei}} \frac{Z_i}{4\pi\epsilon_0|\mathbf{r}_i - \mathbf{r}|} + \int \frac{\rho(\mathbf{r}')}{4\pi\epsilon_0|\mathbf{r}' - \mathbf{r}|}\, d\mathbf{r}' \quad (27)$$

where ρ is the electronic charge distribution determined from the molecular wave function.

Calculations of the molecular electric potential from ab initio calculations have been applied extensively to small molecular systems; see, for example, ref 164–172. Continuum approximations for solvent have been included with quantum techniques in self-consistent reaction field (SCRF) theories to move ab initio methods out of the gas-phase regime, as in ref 173–176. The complexity of such calculations is prohibitive for large systems, but new techniques and approximations combined with ever more powerful computers open doors continually to new possibilities.

IV. Concluding Remarks

The array of methods is quite large and no one method is perfect for all applications. For any given amount of computing power, a hierarchy of models, as described by Friedman,[177] will be necessary to cover the range of problems to be considered. Uniform dielectric models with fixed partial charges will remain the backbone of MD calculations with its speed and simplicity. Effective dielectric models will provide an approximation for solvation when more accurate methods are prohibitive, but they should be approached with caution. The Born energy provides a convenient approximation for solvation energies for roughly spherical bodies and serves to correct for electrostatic cutoffs in MD simulations. Similarly, Debye–Hückel theory provides a convenient approximation for such cases when counterion effects are of interest. For globular molecules with irregular charge distributions, the model of Kirkwood, Westheimer, and Tanford with modifications provides a methodology for calculating intramolecular interactions with a good degree of accuracy. All of the previous methods also share the fact that their analytic form makes them amenable to use in other analytic theories. Numerical techniques allow for the consideration of more detailed effects, not the least of which is the irregular shape of the molecules. They achieve this, however, at the expense of computation

speed. Finite element methods will allow for a very accurate description of the field but are complicated to implement. They will be most useful when a very detailed description of the near field is important, but the bookkeeping of looking up potentials will not make them the most efficient for BD simulations. Finite difference techniques, on the other hand, gain the advantage of trivial look-up by sacrificing the precision of the surface description and the point nature of the charges. But, since the surface of the molecule and point nature of the charges are rather arbitrary constructions and do not have a strong physical basis, the more accurate calculations from finite element techniques may not provide additional physical insight. Inducible dipole models will serve to improve MD calculations by including polarizability. If iteration to convergence is required, however, the calculation may prove prohibitive in the near term. Techniques beyond the PB equation will provide even more accurate models for large molecules in solvent in the future but are currently limited to simple or simplified systems and still face some difficulties matching certain experimental quantities. Quantum mechanical methods will remain limited to fairly small systems and will serve to provide charges and polarizabilities for classical models of larger systems for some time yet.

Thus it is fortunate that such a plethora of approaches exists. Different methods are available for the different levels of accuracy required and different levels of computational power available. Neither is the field closed to new ideas. There are realms where new and innovative ideas may sweep aside current standard approximations. Meanwhile, applications for existing methods abound.

Acknowledgments. We thank Prof. Peter C. Jordan, Prof. Ronald M. Levy, Dr. Jeffry D. Madura, and Prof. B. Montgomery Pettitt for helpful discussions and the reviewers for their useful suggestions. This work has been supported by the National Institutes of Health, the National Science Foundation, the Robert A. Welch Foundation, The Texas Advanced Research Program, the National Center for Supercomputing Applications, the San Diego Supercomputer Center, the Houston Area Research Center, and HNS Supercomputers. J.A.M. is the recipient of the 1987 George Herbert Hitchings Award from the Burroughs Wellcome Fund.

References

(1) Berg, O. G.; von Hipple, P. H. *Ann. Rev. Biophys. Biophys. Chem.* **1985**, *14*, 131–160.
(2) Calef, D. F.; Deutch, J. M. *Ann. Rev. Phys. Chem.* **1983**, *34*, 493–524.
(3) Knowles, J. R.; Albery, W. J. *Acc. Chem. Res.* **1977**, *10* (4), 105.
(4) Ermak, D. L.; McCammon, J. A. *J. Chem. Phys.* **1978**, *69*, 1352.
(5) Northrup, S. H.; Allison, S. A.; McCammon, J. A. *J. Chem. Phys.* **1984**, *80*, 1517.
(6) Northrup, S. H.; Boles, J. O.; Reynolds, J. C. L. *J. Phys. Chem.* **1987**, *91*, 5991–5998.
(7) Allison, S. A.; McCammon, J. A. *Biopolymers* **1984**, *23*, 363–375.
(8) Allison, S. A. *Macromolecules* **1986**, *19*, 118–124.
(9) Lewis, R. J.; Allison, S. A.; Eden, D.; Pecora, R. *J. Chem. Phys.* **1988**, *89* (4), 2490–2503.
(10) McCammon, J. A.; Bacquet, R. J.; Allison, S. A.; Northrup, S. H. *Faraday Discuss. Chem. Soc.* **1987**, *83*, 213.
(11) Allison, S.; Austin, R.; Hogan, M. *J. Chem. Phys.* **1989**, *90* (7), 3843–3854.
(12) Warshel, A.; Russell, S. T. *Q. Rev. Biophys.* **1984**, *17* (3), 283–422.
(13) Matthew, J. B. *Ann. Rev. Biophys. Biophys. Chem.* **1985**, *14*, 387–417.
(14) Rogers, N. K. *Prog. Biophys. Mol. Biol.* **1986**, *48*, 37–66.
(15) Neumann, E. *Prog. Biophys. Mol. Biol.* **1986**, *47*, 197–231.
(16) Honig, B. H. *Ann. Rev. Biophys. Biophys. Chem.* **1986**, *15*, 163–193.
(17) Harvey, S. C. *Proteins* **1989**, *5*, 78–92.
(18) Case, D. A. *Prog. Biophys. Mol. Biol.* **1988**, *52*, 39–70.
(19) Whittaker, E. *A History of the Theories of Aether and Electricity: The Classical Theories*; Philosophical Library Inc.: New York, 1951.
(20) Stillinger, F. H. *J. Chem. Phys.* **1979**, *71*, 1647.
(21) Teleman, O.; Ahlström, P. *J. Am. Chem. Soc.* **1986**, *108*, 4333–4341.
(22) Allen, M. P.; Tildesley, D. J. *Computer Simulation of Liquids*; Oxford University Press: New York, 1987.
(23) Pollock, E. L.; Alder, B. J.; Pratt, L. R. *Proc. Natl. Acad. Sci. U.S.A.* **1980**, *77* (1), 49–51.
(24) Alder, B. J.; Pollock, E. L. *Ann. Rev. Phys. Chem.* **1981**, *32*, 311–329.
(25) de Leeuw, S. W.; Perram, J. W.; Smith, E. R. *Ann. Rev. Phys. Chem.* **1986**, *37*, 245–270.
(26) Smith, E. R.; Wielopolski, P. A. *Mol. Phys.* **1987**, *61*, 1063–1076.
(27) Anderson, J.; Ullo, J. J.; Yip, S. *J. Chem. Phys.* **1987**, *87* (3), 1726–1732.
(28) Alper, H. E.; Levy, R. M. *J. Chem. Phys.* **1989**, *91* (2), 1242–1251.
(29) Barnes, P.; Finney, J. L.; Nicholas, J. D.; Quinn, J. E. *Nature* **1979**, *282*, 459.
(30) Lybrand, T. P.; Kollman, P. A. *J. Chem. Phys.* **1985**, *83* (6), 2923–2933.
(31) Wojcik, M.; Clementi, E. *J. Chem. Phys.* **1986**, *84*, 5970.
(32) Murrell, J. N.; Hassani, N. M. R.; Hudson, B. *Mol. Phys.* **1987**, *60* (6), 1343–1355.
(33) Rullman, J. A. C.; van Duijnen, P. T. *Mol. Phys.* **1988**, *63*, 451.
(34) Sprick, M.; Klein, M. L. *J. Chem. Phys.* **1988**, *89*, 7556.
(35) Straatsma, T. P.; McCammon, J. A. *Mol. Simulat.* **1990**, *5*.
(36) Straatsma, T. P.; McCammon, J. A. *Chem. Phys. Lett.* **1990**, *166*.
(37) Venanzi, C. A.; Manboodiri, K. *Anal. Chim. Acta* **1988**, *210*, 151–162.
(38) Náray-Szabó, G. *J. Mol. Graphics* June 1989, *7*, 76–81.
(39) Brant, D. A.; Miller, W. G.; Flory, P. J. *J. Mol. Biol.* **1967**, *23*, 47–65.
(40) Weill, G.; Andre, J. J. *Biopolymers* **1978**, *17*, 811–814.
(41) Hol, W. G. J.; Halie, L. M.; Sander, C. *Nature* **1981**, *294*, 532–536.
(42) Rao, G. S.; Tyagi, R. S.; Mishra, R. K. *J. Theor. Biol.* **1981**, *90*, 377–389.
(43) Wada, A.; Nakamura, H.; Sakamoto, T. *J. Phys. Soc. Jpn.* **1985**, *54* (10), 4042–4046.
(44) Nakamura, H.; Wada, A. *J. Phys. Soc. Jpn.* **1985**, *54* (10), 4047–4052.
(45) Hammarström, L.; Liljefors, T.; Gasteiger, J. *J. Comput. Chem.* **1988**, *9* (4), 424–440.
(46) Wells, J. A.; Powers, D. B.; Bott, R. R.; Graycar, T. P.; Estell, D. A. *Proc. Natl. Acad. Sci. U.S.A.* **1987**, *84*, 1219–1223.
(47) Nichols, H.; Becktel, W. J.; Mathews, B. W. *Nature* **1988**, *336*, 651–656.
(48) Wierenga, R. K.; Maeyer, M. C. H. D.; Hol, W. G. J. *Biochemistry* **1985**, *24*, 1346–1357.
(49) Sheridan, R. P.; Allen, L. C. *Biophys. Chem.* **1980**, *11*, 133–136.
(50) Koppenol, W. H.; Margoliash, E. *J. Biol. Chem.* **1982**, *257* (8), 4426–4437.
(51) Klapper, I.; Hagstrom, R.; Fine, R.; Sharp, K.; Honig, B. *Proteins* **1986**, *1*, 47–59.
(52) Sharp, K.; Fine, R.; Schulten, K.; Honig, B. *J. Phys. Chem.* **1987**, *91*, 3624–3631.
(53) Rees, D. C. *J. Mol. Biol.* **1980**, *141*, 323–326.
(54) Hill, T. L. *J. Phys. Chem.* **1956**, *60*, 253–255.
(55) Fersht, A. R.; Sternberg, M. J. E. *Protein Eng.* **1989**, *2* (7), 527–530.
(56) Hopfinger, A. J. *Conformational Properties of Macromolecules*; Academic Press: New York, 1973.
(57) McCammon, J. A.; Harvey, S. C. *Dynamics of Proteins and Nucleic Acids*; Cambridge University Press: Cambridge, 1987.
(58) Wendoloski, J. J.; Matthew, J. B. *Proteins* **1989**, *5*, 313–321.
(59) Northrup, S. H.; Pear, M. R.; Morgan, J. D.; McCammon, J. A.; Karplus, M. *J. Mol. Biol.* **1981**, *153*, 1087–1109.
(60) Levitt, M. *Cold Springs Harbor Symp. Quant. Biol.* **1983**, *47*, 251–262.
(61) Born, M. *Z. Phys.* **1920**, *1*, 45–48.
(62) (a) Latimer, W. M.; Pitzer, K. S.; Slansky, C. M. *J. Chem. Phys.* **1939**, *7*, 108–111. (b) Rashin, A. A.; Honig, B. *J. Phys.*

Chem. **1985**, *89*, 5588–5593. (c) Hirata, F.; Redfern, P.; Levy, R. M. *Int. J. Quantum Chem.: Quantum Biol. Symp.* **1988**, *15*, 179–190.
(63) Straatsma, T. P.; Berendsen, H. J. C. *J. Chem. Phys.* **1988**, *89*, 5876–5886.
(64) Debye, V. P.; Hückel, E. *Phys. Z.* **1923**, *24*, 185–206.
(65) Allison, S. A.; Bacquet, R. J.; McCammon, J. A. *Biopolymers* **1988**, *27*, 251.
(66) Kirkwood, J. G. *J. Chem. Phys.* **1934**, *2* (7), 351–361.
(67) Kirkwood, J. G.; Westheimer, F. H. *J. Chem. Phys.* **1938**, *6*, 506–512.
(68) Westheimer, F. H.; Kirkwood, J. G. *J. Chem. Phys.* **1938**, *6*, 513–517.
(69) Tanford, C.; Kirkwood, J. G. *J. Am. Chem. Soc.* **1957**, *79* (20), 5333–5339.
(70) Tanford, C. *J. Am. Chem. Soc.* **1957**, *79* (20), 5340–5347.
(71) Tanford, C. *J. Am. Chem. Soc.* **1957**, *79* (20), 5348–5352.
(72) Tanford, C.; Roxby, R. *Biochemistry* **1972**, *11* (11), 2192–2198.
(73) Shire, S. J.; Hanania, G. I. H.; Gurd, F. R. N. *Biochemistry* **1974**, *13* (14), 2967–2974.
(74) Shire, S. J.; Hanania, G. I. H.; Gurd, F. R. N. *Biochemistry* **1974**, *13* (14), 2974–2979.
(75) Matthew, J. B.; Richards, F. M. *Biopolymers* **1984**, *23*, 2743–2759.
(76) Delepierre, M.; Dobson, C. M.; Karplus, M.; Poulson, F. M.; States, D. J.; Wedin, R. E. *J. Mol. Biol.* **1987**, *197*, 111–130.
(77) Head-Gordon, T.; Brooks, C. L. *J. Phys. Chem.* **1987**, *91*, 3342.
(78) van Faassen, E. E.; Mofers, F. J. M.; Casteleijn, G. *J. Chem. Phys.* **1980**, *73* (3), 1354–1358.
(79) Brunschwig, B, S.; Ehrenson, S.; Sutin, N. *J. Phys. Chem.* **1987**, *91*, 4714–4723.
(80) Imoto, T. *Biophys. J.* **1983** *44*, 293–298.
(81) Head-Gordon, T.; Brooks, C. L., III. *J. Phys. Chem.* **1989**, *93*, 490–494.
(82) Northrup, S. H.; Reynolds, J. C. L.; Miller, C. M.; Forrest, K. J.; Boles, J. O. *J. Am. Chem. Soc.* **1986**, *108*, 8162–8170; **1987**, *109*, 3176.
(83) Orttung, W. H. *Ann. N.Y. Acad. Sci.* **1977**, *303*, 22.
(84) Axelsson, O.; Barker, V. A. *Finite Element Solution of Boundary Value Problems*; Academic Press: Orlando, 1984.
(85) McAllister, D.; Smith, J. R.; Diserens, N. J. *Computer Modelling in Electrostatics*; Wiley: New York, 1985.
(86) Joe, B. *SIAM J. Sci. Stat. Comput.* **1989**, *10* (4), 718.
(87) Perucchio, R.; Saxena, M. *Int. J. Num. Methods Eng.* **1989**, *28*, 2469–2501.
(88) Gatica, G. N. *SIAM J. Num. Anal.* **1988**, *25* (1), 41.
(89) Ainsworth, M.; Zhu, J. Z.; Craig, A. W.; Zienkiewicz, O. C. *Int. J. Num. Methods Eng.* **1989**, *28*, 2161–2174.
(90) Orttung, W. H. *J. Am. Chem. Soc.* **1978**, *100* (14), 4369–4375.
(91) Orttung, W. H.; Vosooghl, D. *J. Phys. Chem.* **1983**, *87*, 1432–1437.
(92) Orttung, W. H.; Jullen, D. S. *J. Phys. Chem.* **1983**, *87*, 1438–1444.
(93) Orttung, W. H. *J. Phys. Chem.* **1985**, *89*, 3011–3016.
(94) Warwicker, J.; Watson, H. C. *J. Mol. Biol.* **1982**, *157*, 671–679.
(95) Edmonds, D. T.; Rogers, N. K.; Sternberg, M. J. E. *Mol. Phys.* **1984**, *52* (6), 1487–1494.
(96) Gilson, M. K.; Sharp, K. A.; Honig, B. H. *J. Comput. Chem.* **1987**, *9* (4), 327–335.
(97) Sines, J. J.; Allison, S. A.; Wierzbicki, A.; McCammon, J. A. *J. Phys. Chem.*, in press.
(98) Northrup, S. H.; Luton, J. A.; Boles, J. O.; Reynolds, J. C. L. *J. Computer-Aided Mol. Des.* **1987**, *1*, 291–311.
(99) Madura, J. D.; McCammon, J. A. *J. Phys. Chem.* **1989**, *93*, 7285–7287.
(100) Gilson, M. K.; Honig, B. H. *Proteins* **1988**, *3*, 32–52.
(101) Bashford, D.; Karplus, M.; Canters, G. W. *J. Mol. Biol.* **1988**, *203*, 507–510.
(102) Gilson, M. K.; Honig, B. *Proc. Natl. Acad. Sci. U.S.A.* **1989**, *86*, 1524–1528.
(103) Gilson, M. K.; Honig, B. *Proteins* **1988**, *4*, 7–18.
(104) Rogers, N. K.; Moore, G. R.; Sternberg, M. J. E. *J. Mol. Biol.* **1985**, *182*, 613–616.
(105) Warwicker, J. *J. Theor. Biol.* **1986**, *121*, 199–210.
(106) Warwicker, J. *J. Mol. Biol.* **1989**, *206*, 381–395.
(107) Warwicker, J.; Ollis, D.; Richards, F. M.; Steitz, T. A. *J. Mol. Biol.* **1985**, *186*, 645–649.
(108) Pickersgill, R. W.; Goodenough, P.; Sumner, I. G.; Collins, M. E. *Biochem. J.* **1988**, *254*, 235–238.
(109) Dao-Pin, S.; Liao, D.; Remington, S. J. *Proc. Natl. Acad. Sci.* **1989**, *86*, 5361–5365.
(110) Levitt, D. G. *Biophys. J.* **1978**, *22*, 209–219.
(111) Zauhar, R. J.; Morgan, R. S. *J. Comput. Chem.* **1988**, *9* (2), 171–187.
(112) Zauhar, R. J.; Morgan, R. S. *J. Mol. Biol.* **1985**, *186*, 815–820.
(113) Rashin, A. A.; Namboodiri, K. *J. Phys. Chem.* **1987**, *91*, 6003–6012.
(114) Drummond, M. L. J. *J. Chem. Phys.* **1988**, *88* (8), 5014–5020.
(115) Drummond, M. L. J. *J. Chem. Phys.* **1988**, *88* (8), 5021–5026.
(116) Jordan, P. C. *Biophys. J.* **1982**, *39*, 157–164.
(117) Jordan, P. C. *Biophys. J.* **1983**, *41*, 189–195.
(118) Jordan, P. C. *Biophys. J.* **1984**, *45*, 1091–1100.
(119) Jordan, P. C. *Biophys. J.* **1984**, *45*, 1101–1107.
(120) Jordan, P. *Biophys. J.* **1987**, *51*, 297–311.
(121) Rashin, A. A. *Int. J. Quantum Chem.* **1988**, *15*, 113–118.
(122) Jackson, J. D. *Classical Electrodynamics*, 2nd ed.; Wiley: New York, 1975.
(123) Shaw, P. B. *Phys. Rev. A* **1985**, *32* (4), 2476–2487.
(124) Shaw, P. B. *Phys. Rev. A* **1987**, *35* (5), 2254–2265.
(125) Krishtalik, L. I.; Topalev, V. V. *Mol. Biol. U.S.S.R.* **1984**, *18*, 892–900 (pp 721–728 (1985) in translation).
(126) Warshel, A.; Levitt, M. *J. Mol. Biol.* **1976**, *103*, 227–249.
(127) Warshel, A.; Russell, S. T.; Churg, A. K. *Proc. Natl. Acad. Sci.* **1984**, *81*, 4785–4789.
(128) Van Belle, D.; Couplet, I.; Prevost, M.; Wodak, S. J. *J. Mol. Biol.* **1987**, *198* (4), 721–735.
(129) Berendsen, H. J. C.; Grigera, J. R.; Straatsma, T. P. *J. Phys. Chem.* **1987**, *91*, 6269–6273.
(130) Adams, D. J.; Dubey, G. S. *J. Comput. Phys.* **1987**, *72* (1), 156–176.
(131) Nakamura, H. *J. Phys. Soc. Jpn.* **1988**, *57* (11), 3702–3705.
(132) Davis, M. E.; McCammon, J. A. *J. Comput. Chem.* **1989**, *10* (3), 386–391.
(133) Meijerink, J. A.; van der Vorst, H. A. *J. Comput. Phys.* **1981**, *4*, 134–155.
(134) Kightley, J. R.; Thompson, C. P. *SIAM J. Sci. Stat. Comput.* **1987**, *8* (5), 701–715.
(135) Ashcraft, C. C.; Grimes, R. G. *SIAM J. Sci. Stat. Comput.* **1988**, *9* (1), 122–151.
(136) Vorst, H. A. V. D. *SIAM. J. Sci. Stat. Comput.* **1989**, *10* (6), 1174–1185.
(137) Davis, M. E.; McCammon, J. A. *J. Comput. Chem.* **1990**, *11* (3), 000–000.
(138) Jayaram, B.; Sharp, K.; Honig, B. *Biopolymers* **1989**, *28*, 975–993.
(139) Jordan, P. C.; Bacquet, R. J.; McCammon, J. A.; Tran, P. *Biophys. J.* **1989**, *55*, 1041–1052.
(140) Allison, S. A.; Sines, J. J.; Wierzbicki, A. *J. Phys. Chem.* **1989**, *93*, 5819–5823.
(141) Bacquet, R. J.; McCammon, J. A.; Allison, S. A. *J. Phys. Chem.* **1988**, *92*, 7134–7141.
(142) Onsager, L. *Chem. Rev.* **1933**, *13*, 73–89.
(143) Gilson, M. K.; Rashin, A.; Fine, R.; Honig, B. *J. Mol. Biol.* **1985**, *183*, 503–516.
(144) Oxtoby, D. W. *J. Chem. Phys.* **1980**, *72*, 5171–5176.
(145) Nakamura, H.; Sakamoto, T.; Wada, A. *Protein Eng.* **1988**, *2* (3), 177–183.
(146) Ehrenson, S. *J. Comput. Chem.* **1989**, *10* (1), 77–93.
(147) Rossky, P. J. *Ann. Rev. Phys. Chem.* **1985**, *63*, 321–346.
(148) Pettitt, B. M.; Rossky, P. J. *J. Chem. Phys.* **1986**, *84* (10), 5837–5844.
(149) Pettitt, B. M.; Karplus, M. *J. Phys. Chem.* **1988**, *92*, 3994–3997.
(150) Bratko, D.; Friedman, H. L.; Zhong, E. C. *J. Chem. Phys.* **1986**, *85* (1), 377–384.
(151) Bacquet, R.; Rossky, P. J. *J. Chem. Phys.* **1983**, *79* (3), 1419–1426.
(152) Bacquet, R.; Rossky, P. J. *J. Phys. Chem.* **1984**, *88*, 2660–2669.
(153) Hirata, F.; Levy, R. M. *J. Phys. Chem.* **1989**, *93*, 479–484.
(154) Murthy, C. S.; Bacquet, R. J.; Rossky, P. J. *J. Phys. Chem.* **1985**, *89*, 701–710.
(155) Patey, G. N. *J. Chem. Phys.* **1980**, *72* (10), 5763–5771.
(156) Bratko, D.; Vlachy, V. *Chem. Phys. Lett.* **1982**, *90* (6), 434–438.
(157) Outhwaite, C. W. *J. Chem. Soc., Faraday Trans. 2* **1986**, *82*, 789–794.
(158) Outhwaite, C. W.; Bhuiyan, L. B. *J. Chem. Phys.* **1986**, *84* (6), 3461.
(159) Attard, P.; Mitchell, D. J.; Ninham, B. W. *J. Chem. Phys.* **1988**, *88* (8), 4987–4996.
(160) Bratko, D. *Bioelectrochem. Bioenerg.* **1984**, *13*, 459–471.
(161) Bratko, D.; Bhuiyan, L. B.; Outhwaite, C. W. *J. Phys. Chem.* **1986**, *90*, 6248–6251.
(162) Szabo, A.; Ostlund, N. S. *Modern Quantum Chemistry*; Macmillan: New York, 1982.
(163) Hehre, W. J.; Radom, L.; v R. Schleyer, P.; Pople, J. A. *Ab Initio Molecular Orbital Theory*; Wiley: New York, 1986.
(164) Politzer, P.; Truhlar, D. G. *Chemical Applications of Atomic and Molecular Electrostatic Potentials*; Plenum Press: New York, 1981.
(165) Boudon, A.; Chretien, J. R. *C. R. Seances Acad. Sci.* **1988**, *307*, 505–510.
(166) Goursot, A.; Fajula, F.; Weber, J. *J. Phys. Chem.* **1988**, *92*, 4456–4461.
(167) Luque, L.; Sanz, F.; Illas, F.; Pouplana, R.; Smeyers, Y. G. *Eur. J. Med. Chem.* **1988**, *23*, 7–10.
(168) Venanzi, T. J.; Venanzi, C. A. *J. Med. Chem.* **1988**, *31*,

1879–1885.
(169) Williams, D. E. *J. Comput. Chem.* **1988**, *9* (7), 745–763.
(170) Pepe, G.; Reboul, J.; Oddon, Y. *Eur. J. Med. Chem.* **1989**, *24*, 1–13.
(171) Norinder, U.; Hogberg, T. *Acta Pharm. Nord.* **1989**, *2* (1), 75–88.
(172) Orozco, M.; Luque, F. J. *Chem. Phys. Lett.* **1989**, *160* (3), 305–310.
(173) Hoshi, H.; Sakurai, M.; Inoue, Y.; Chujo, R. *J. Mol. Struct.* **1988**, *180*, 267–281.
(174) Mikkelsen, K. V.; Agren, H.; Jensen, H. J. A.; Helgaker, T. *J. Chem. Phys.* **1988**, *89* (5), 3086–3095.
(175) Aguilar, M. A.; Valle, F. J. O. D. *Chem. Phys.* **1989**, *129*, 439–450.
(176) Frecer, V.; Majekova, M.; Miertus, S. *J. Mol. Struct.* **1989**, *183*, 403–419.
(177) Friedman, H. L. *Pure Appl. Chem.* **1981**, *53*, 1277–1290.